

Chirality assignments in carbon nanotubes based on resonant Raman scattering

C. Thomsen^{*,1}, H. Telg¹, J. Maultzsch¹, and S. Reich²

¹ Institut für Festkörperphysik, Technische Universität Berlin, Hardenbergstr. 36, 10623 Berlin, Germany

² Departement of Engineering, University of Cambridge, United Kingdom

Received 11 October 2004, revised 30 May 2005, accepted 30 May 2005

Published online 29 June 2005

PACS 61.46.+w, 73.22.-f, 78.30.-j, 81.07.De

Resonant Raman scattering is a well-known method for investigating the optical transitions in solids [1]. Here we show that the fully symmetric radial breathing mode (RBM) of carbon nanotubes can be used to derive an assignment of their chiral indices. Our assignment is based on a plot of the resonance maxima for the radial breathing modes as a function of laser excitation energy *versus* inverse ω_{RBM} , a so-called Kataura plot. Different from recent luminescence measurements [2], the chirality of both semiconducting and metallic nanotubes can be investigated.

© 2005 WILEY-VCH Verlag GmbH & Co. KGaA, Weinheim

1 Introduction

The experimental determination of the chiral indices of single-walled carbon nanotubes has been a challenge ever since their discovery [3]. Given the integers n_1 and n_2 , the chiral vector $\mathbf{c} = n_1\mathbf{a}_1 + n_2\mathbf{a}_2$, which determines all topological properties of the nanotubes, is known, including their transport characteristics, i.e., whether they are semiconducting or metallic [4]. For all applications of these fascinating one-dimensional systems the determination of the chiral indices is thus a must.

There have been a number of experimental approaches based on TEM [5], STM [6], or the radial breathing mode in Raman spectroscopy [4] to determine the diameter of a given nanotube. In principle, an exact knowledge of the diameter allows the (nearly unique) determination of the chiral indices of a tube from the relation

$$d = \frac{a_0}{\pi} \sqrt{n_1^2 + n_1 n_2 + n_2^2}, \quad (1)$$

where $a_0 = (2.462 \pm 0.002) \text{ \AA}$ [7]. In practice, however, the diameters are too closely spaced for such a procedure to work: A sample grown with a diameter range of 1.0–1.5 nm can contain up to around 125 different chirality tubes. Knowing a particular tube diameter to within, say 10% as is typical for TEM or STM, still leaves 30 different chiral index pairs to assign to one experimental diameter. Knowing a chiral index pair is important, however, for a number of application-related reasons, the most important one being the systematic dependence of the transport characteristic on chiral indices. Whenever $(n_1 - n_2) \bmod 3 = 0$ a nanotube is metallic, otherwise it is semiconducting. This – at first sight curious – relation is straightforwardly explained by the bandstructure of graphene, a single layer of graphite, see Fig. 1. Rolling a sheet to a tube corresponds to generating lines in the Brillouin zone of graphene as indicated in the figure (*left*). Depending on whether or not these lines run through the K-point, where valence and conduction

* Corresponding author: e-mail: thomsen@physik.tu-berlin.de, Phone: +49 30 314 23 187, Fax: +49 30 314 277 705

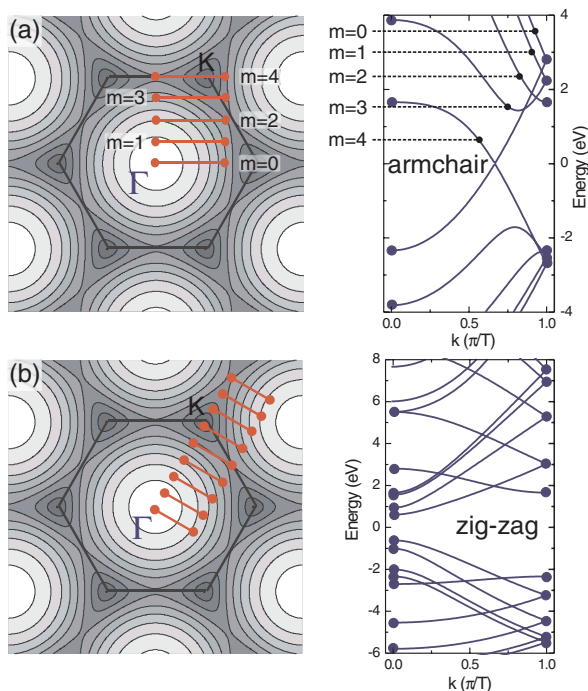


Fig. 1 (online colour at: www.pss-b.com) (a) Left: Brillouin zone of a two-dimensional graphene sheet. The lines are the Brillouin zone of a tube rolled up in the so-called armchair direction. Right: The electronic bandstructure along the lines on the left. (b) Corresponding plots of a tube rolled up in the zig-zag direction. The upper tube is metallic, the lower one semiconducting.

bands cross, the nanotube is metallic (*upper*) or semiconducting (*lower*), as is evident from the calculated bandstructures (*right*) obtained from a third-order tight-binding calculation [8].

The ability to resolve chiral indices by Raman spectroscopy is improved dramatically by explicitly taking into account the transition energies of the singularities in the density of electronic states. The radial breathing mode is only seen in the spectra in or near such a singularity. In the past, attempts to find the chiral indices in this way were hampered by the fact that the actual transition energies were taken from too simple models to interpret quantitatively experimental data [9]. The so-determined chiral indices were highly dependent on the (somewhat arbitrary) choice of a model parameter, namely the value of the overlap integral γ_0 in the first-order tight-binding description of graphene.

2 Luminescence

A significant advance in the field was brought about by the preparation of isolated single-walled carbon nanotubes in such a way that they would not rebundle after ultrasonification by wrapping them with a layer of SDS [2]. In luminescence experiments on such tubes the distinct energies of many different tubes were found. In bundled tubes, on the other hand, tunneling of carriers into neighboring metallic tubes quenched the luminescence, which is relatively long lived in isolated tubes (lifetime ≥ 40 ps) [10]. Based on the theoretical work of Reich et al. [8], which provided an improved tight-binding parametrization of the electronic energies and their dependence on chiral index, Bachilo et al. found a successful assignment of about 30 different semiconducting tubes [2].

3 Resonant Raman

The luminescence work was followed by resonance Raman spectroscopy, employing the density-of-states singularities for an enhancement of the Raman cross section [11–14]. In Fig. 2 we show the low-energy part of several Raman spectra excited with nearby wavelengths of a dye laser, dispersed by a Dilor-XY triple Raman spectrometer and recorded by a charged-coupled device. Nicely seen are the

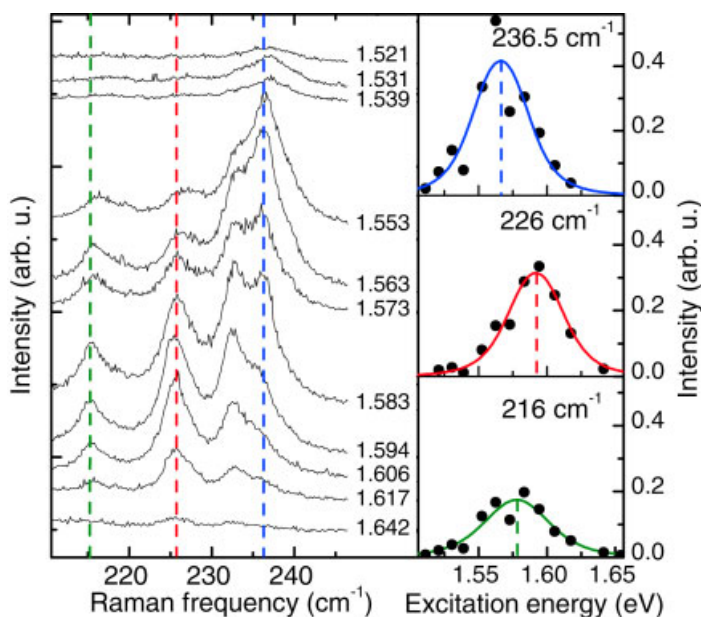


Fig. 2 (online colour at: www.pss-b.com) Left: Resonance Raman spectra of the radial breathing mode excited with various laser energies of a Ti:Sa laser as indicated. Clearly seen is the *laola*-type shift of the maximum intensity through the spectra. Right: Resonance curves of three selected radial breathing modes. The resonance maxima occur apparently at a different energy.

peaks of the radial breathing mode, which go through a resonance maximum as a function of laser energy. Different breathing modes have their maximum intensity at systematically varying energies, forming *laola*-like waves in the Raman spectra [15]. This behavior is seen in the shift of the three resonance curves plotted on the right of Fig. 2; the maximum (blue) of the RBM mode at 236 cm^{-1} shifts first up to higher energies (red) for the mode at 226 cm^{-1} and then back down to lower energies (green) for $\omega_{\text{RBM}} = 216\text{ cm}^{-1}$. As we shall see later, the curvature of the branches in the so-called Kataura plot is responsible for this effect. All three RBM modes correspond to different-chirality nanotubes; the challenge is to find out *to which* chirality a specific RBM-resonance peak belongs.

Using a pattern-recognition technique related to the one employed by Bachilo et al. [2], we obtained a one-to-one correspondence of the experimental inverse RBM frequency and d in a diameter-*versus*-transition-energy plot, see Fig. 3. The pattern recognition is performed by stretching and shifting the upper *versus* lower horizontal axes until good correspondence between the experimental points and the calculated values is achieved. Physically speaking, applying this procedure to the x -axis corresponds to changing the constants c_1 and c_2 in the well-known diameter- ω_{RBM} frequency relationship [4, 16]

$$\omega_{\text{RBM}} = \frac{c_1}{d} + c_2. \quad (2)$$

Stretching the y -axis corresponds to adjusting the energy parameters in the theoretical model.

It turns out that due to the different number of tubes within the so-called branches the assignment in Fig. 3 (left) is unique. Shifting only slightly upper and lower axes with respect to each other is not possible because it brings experiment and theory out of registry. Displacing the experiment by an entire branch, as is demonstrated in Fig. 3 (right), is also impossible without losing the correct count of nanotubes within a branch. This is best seen for the (9, 1) and (11, 0) branches (highlighted area). The former consists of three nanotubes, the latter of four, and in the shifted plot one tube is missing in both branches as compared to theory (vertical bars). A similar argument holds for a shift to the left (not shown), making the assignment in Fig. 3 indeed the only possible one.

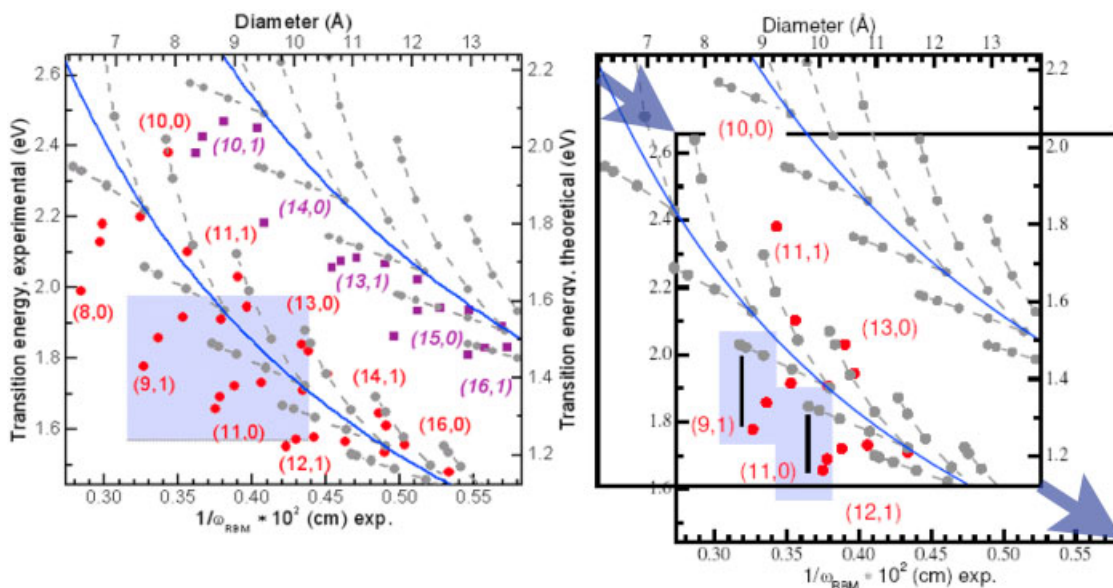


Fig. 3 (online colour at: www.pss-b.com) Left: Kataura plot of the experimental resonance maxima vs. inverse ω_{RBM} , compared to third-order tight-binding calculated transition energies vs. nanotube diameter. The branches are labeled by their outermost nanotube, which has the smallest possible chiral angle in a branch. Neighboring tubes in a branch have the indices $(n_1 - 1, n_2 + 2)$ for $n_1 \geq n_2$. The lower transitions (red, circles) are experimental points belonging to E_{22}^S , the upper ones (magenta, squares) to E_{11}^M . Theoretical points are light grey. Highlighted are the (9, 1) and the (11, 0) branches. Right: A shift of the assignment by an entire branch (arrows) renders an incorrect count of the number of nanotubes, see text (only a subset of the data is shown for clarity). After Ref. [14].

The constants c_1 and c_2 were thus determined experimentally and independent of assumptions other than the general validity of Eq. (2). Best values for the constants are $c_1 = (214.4 \pm 2) \text{ cm}^{-1} \text{ nm}$ and $c_2 = (18.7 \pm 2) \text{ cm}^{-1}$, quite different from previous work. In fact, the deviations to older c_1 and c_2 values [9, 17] are so large that this new work renders previous Raman-based assignments invalid. Recently, in a study of the effect of laser heating our assignment was confirmed by a different group [18].

4 Summary

From a comparison of ≈ 40 different-chirality nanotubes to third-order tight-binding calculations we are able to derive the parameters of the well-known inverse relationship between the breathing-mode frequency ω_{RBM} of a nanotube and its diameter d , independent of any prior assumptions [13, 14]. We find $\omega_{\text{RBM}} = (214 \pm 2) \text{ cm}^{-1} \text{ nm}/d + (19 \pm 2) \text{ cm}^{-1}$. Our measurements confirm the importance of the so-called nanotubes branches and allow an assignment of all observed tubes to specific chiral indices.

Acknowledgements We are grateful to F. Hennrich (Forschungszentrum Karlsruhe) for providing the samples used in this work. SR thanks the Oppenheimer Funds and Newnham College for financial support.

References

- [1] M. Cardona, in: *Light Scattering in Solids II*, Topics in Applied Physics Vol. 50, edited by M. Cardona and G. Güntherodt (Springer, Berlin, 1982), p. 19.
- [2] S. M. Bachilo, M. S. Strano, C. Kittrell, R. H. Hauge, R. E. Smalley, and R. B. Weisman, *Science* **298**, 2361 (2002).
- [3] S. Iijima and T. Ichihashi, *Nature* **363**, 603 (1993).
- [4] S. Reich, C. Thomsen, and J. Maultzsch, *Carbon Nanotubes: Basic Concepts and Physical Properties* (Wiley-VCH, Weinheim, 2004), p. 141.

- [5] C. Qin and L.-M. Peng, *Phys. Rev. B* **65**, 155431 (2002).
- [6] L. C. Venema, V. Meunier, Ph. Lambin, and C. Dekker, *Phys. Rev. B* **62**, 2991 (2000).
- [7] Y. X. Zhao and I. L. Spain, *Phys. Rev. B* **40**, 993 (1989).
- [8] S. Reich, J. Maultzsch, C. Thomsen, and P. Ordejón, *Phys. Rev. B* **66**, 035412 (2002).
- [9] A. Jorio, R. Saito, J. H. Hafner, C. M. Lieber, M. Hunter et al., *Phys. Rev. Lett.* **86**, 1118 (2001).
- [10] S. Reich, M. Dworzak, A. Hoffmann, C. Thomsen, and M. S. Strano, *Phys. Rev. B* **71**, 033402 (2005).
- [11] M. S. Strano, S. K. Doorn, E. H. Haroz, C. Kittrell, R. Hauge, and E. Smalley, *Nano Lett.* **3**, 1091 (2003).
- [12] S. K. Doorn, D. A. Heller, P. W. Barone, M. L. Usrey, and M. S. Strano, *Appl. Phys. A* **78**, 1147 (2004).
- [13] H. Telg, J. Maultzsch, S. Reich, F. Hennrich, and C. Thomsen, *Molecular Nanostructures*, edited by H. Kuzmany, J. Fink, M. Mehring, and S. Roth, AIP Conference Proceedings Vol. 723 (Melville, New York, 2004), p. 330.
- [14] H. Telg, J. Maultzsch, S. Reich, F. Hennrich, and C. Thomsen, *Phys. Rev. Lett.* **93**, 177401 (2004).
- [15] I. Farkas, D. Helbing, and T. Vicsek, *Nature* **419**, 131 (2002).
- [16] R. A. Jishi, L. Venkataraman, M. S. Dresselhaus, and G. Dresselhaus, *Chem. Phys. Lett.* **209**, 77–82 (1993).
- [17] C. Kramberger, R. Pfeiffer, H. Kuzmany, V. Zolyomi, and J. Kürti, *Phys. Rev. B* **68**, 235404 (2003).
- [18] C. Fantini, A. Jorio, M. Souza, M. S. Strano, M. S. Dresselhaus, and M. A. Pimenta, *Phys. Rev. Lett.* **93**, 147406 (2004).
- [19] V. N. Popov, *New J. Phys.* **6**, 17 (2004).